Herbert L. GINN III

University of South Carolina

CPC based converter control for systems with non-ideal supply voltage

Abstract. *In recent years there have been many strategies proposed such as proportional plus resonant P-R controllers both in the stationary and in the synchronous reference frame that demonstrate grid-connected converter performance can be improved under non-ideal supply conditions such as supply asymmetry and supply voltage distortion. However, when employed in systems with high frequency variability such as micro-grids, the synchronization method required for operation in the synchronous reference frame or for dynamic retuning of the resonant controller may experience poor performance. A method is presented here based on CPC current decomposition that allows control of grid connected converters without direct supply synchronization and that is also suitable for operation under distorted and asymmetrical supply voltage conditions.*

Streszczenie. *W ostatnich latach zaproponowano wiele metod poprawy wydajności przekształtników częstotliwości w warunkach nieidealnego zasilania, w obecności asymetrii i zakłóceń. Jedną z nich z nich jest użycie proporcjonalnych i rezonansowych kontrolerów P-R, pracujących w stacjonarnych i synchronicznych współrzędnych odniesienia. Niestety, takie kontrolery pracujące w warunkach dużej zmienności częstotliwości, która może pojawiać się w mikro-sieciach, z powodu potrzebnej synchronizacji współrzędnych odniesienia lub dynamicznego przestrajania kontrolera rezonansowego, mogą nie pracować zadawalająco. W artykule zaproponowano metodę opartą na rozkładzie prądów według teorii CPC, która pozwala sterować przekształtniki częstotliwości bez bezpośredniej synchronizacji źródeł i nadającą się również do stosowania w obecności odkształceń i asymetrii napięcia zasilania. (**Sterowanie przekształtnikiem częstotliwości oparte na rozkładzie prądów według teorii CPC w układach z nieidealnym źródłami zasilania**)*

Keywords: voltage-source converters, supply synchronization, VSC control.
Słowa kluczowe: napięciowe przekształtniki częstotliwości, synchronizacja źródeł zasilania, sterowanie VSC.

Introduction

In recent years much attention has been given to proportional plus resonant controllers for voltage source converter (VSC) applications due to performance advantages over PI control [1]-[4]. Many strategies have been proposed for use of P-R controllers both in the stationary and in the synchronous reference frame that demonstrate converter performance can be improved under non-ideal supply conditions such as supply asymmetry and supply voltage distortion. However, when employed in systems with high frequency variability such as micro-grids, performance of the synchronization method required for operation must be considered.

In [5] a control method was introduced that does not require direct supply synchronization. However, only frequency variation was considered and results were shown only for VSC based rectifier application. Here the analysis is extended for systems with non-ideal supply voltage including asymmetry and voltage distortion in addition to high supply voltage frequency variation and a reference signal generator is proposed for such conditions.

CPC reference generator without supply voltage synchronization

A CPC based reference signal generator that does not require direct supply synchronization was presented in [6] for systems with small frequency deviations. Analysis was performed for systems with large frequency variation and the method was extended for a limited case in [5]. Here the effect of frequency variation is considered for all possible CPC components at the fundamental frequency.

A CPC reference signal can be based on an efficient recursive discrete Fourier Transform (RDFT) algorithm for computing fundamental components of the measured quantities, a CPC based current decomposition algorithm used to provide separate control of orthogonal current components, and a current reconstruction algorithm to obtain the final reference current [6]. The behavior of each of these three basic reference signal generator subsystems must be analyzed for frequency variation in order to develop a CPC based control without supply synchronization. The results of frequency variation on the RDFT presented in [5] are summarized briefly once again here for completeness.

a. Frequency Variation Effect on RDFT

With the moving-window approach a computationally efficient recursive expression for the DFT can be obtained [7, 8]. To avoid accumulation of errors caused by multiplication rounding, the following expression

$$\begin{aligned}\tilde{\mathbf{X}}_1(k) &= \mathrm{Re}\{\tilde{\mathbf{X}}_1(k)\} + j\,\mathrm{Im}\{\tilde{\mathbf{X}}_1(k)\} \\ &= [\mathrm{Re}\{\tilde{\mathbf{X}}_1(k-1)\} + P(k) - P(k-N)] \\ &+ j[\mathrm{Im}\{\tilde{\mathbf{X}}_1(k-1)\} + Q(k) - Q(k-N)]\end{aligned} \tag{1}$$

was developed in [6], where

$$P(k) = \frac{\sqrt{2}}{N} x(k) \cos \omega_{1g} k \,, \tag{2}$$

$$P(k-N) = \frac{\sqrt{2}}{N} x(k-N) \cos \omega_{1g} k \,, \tag{3}$$

$$Q(k) = \frac{\sqrt{2}}{N} x(k) \sin \omega_{1g} k \,, \text{ and} \tag{4}$$

$$Q(k-N) = \frac{\sqrt{2}}{N} x(k-N) \sin \omega_{1g} k \,. \tag{5}$$

An error in the output of the RDFT occurs when the frequency of the input signal deviates from the nominal frequency generated in the converter control ω_{1g}. That error is the main source of concern for systems with high frequency variability. If the input signal frequency is changed by an amount of $\Delta\omega$, while the sampling clock frequency remains fixed, then the estimated output will contain some errors.

In order to analyze the effects of the error without losing generality, assume that the input signal is a pure sinusoid

$$x = \sqrt{2} A \sin[(\omega_{1g} + \Delta\omega)t + \varphi] \,, \tag{6}$$

where, ω_{1g}, generated by the implementation device, is equal to the nominal frequency of the power system and $\Delta\omega$ expresses the frequency drift. The discrete output of (1), in this case, becomes

$$\begin{aligned}\mathrm{Re}\{\tilde{\boldsymbol{X}}_1(k)\} &= \gamma A\sin[(2\omega_{1g}+\Delta\omega)k-\delta+\varphi] \\ &\quad +\lambda A\sin[(\Delta\omega k)-\delta+\varphi] \\ \mathrm{Im}\{\tilde{\boldsymbol{X}}_1(k)\} &= \gamma A\cos[(2\omega_{1g}+\Delta\omega)k-\delta+\varphi] \\ &\quad -\lambda A\cos[(\Delta\omega k)-\delta+\varphi]\end{aligned} \quad (7)$$

where $\delta=\dfrac{\Delta\omega\pi}{\omega_{1g}}$, $\gamma=\dfrac{\sin\delta}{2\pi+\delta}$ and $\lambda=\dfrac{\sin\delta}{\delta}$.

If the frequency of measured signal x drifts from its nominal frequency ω_{1g} by $\Delta\omega$, then the estimated outputs of the RDFT will involve two frequency components. The first one is a high frequency component. Its frequency is around two times of ω_{1g} with the amplitude of γA. The second one is a low frequency component that mainly determines the features and precisions of the estimated outputs. The estimated magnitude and phase of the measured signal, without considering the effects of the high frequency components, can be written as

$$|\tilde{\boldsymbol{X}}_1(k)|\approx\sqrt{(\mathrm{Re}\{\tilde{\boldsymbol{X}}_1(k)\})^2+(\mathrm{Im}\{\tilde{\boldsymbol{X}}_1(k)\})^2}=\lambda A \quad (8)$$

and

$$Phase\approx-\frac{\pi}{2}+(\Delta\omega k)-\delta+\varphi=\Delta\varphi(k)+\varphi-\frac{\pi}{2}. \quad (9)$$

In order to use the RDFT with fixed reference frequency ω_{1g} for VSC control, the magnitudes of the error factors γ and λ must be within an acceptable level. In order to evaluate these two error factors, Fig. 1 gives the relations of γ ($\Delta\omega/\omega_{1g}$) and $\lambda(\Delta\omega/\omega_{1g})$.

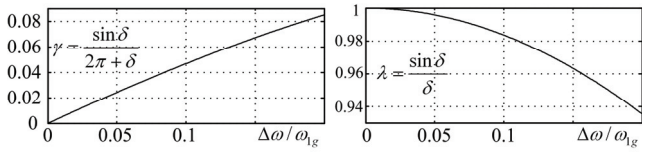

Fig. 1. $\gamma(\Delta\omega/\omega_{1g})$ and $\lambda(\Delta\omega/\omega_{1g})$.

b. Frequency variation effect on CPC based current decomposition

An orthogonal decomposition appropriate for most grid-connected VSC applications is provided by the CPC theory [9]. For sinusoidal conditions, current can be decomposed into active, reactive and unbalanced components. In order to perform this decomposition the system, as seen from the point of measurement, is expressed in terms of two admittances, the equivalent admittance and the unbalanced admittance. The equivalent admittance is expressed as

$$\boldsymbol{Y}_e=G_e+jB_e=\boldsymbol{Y}_{RS}+\boldsymbol{Y}_{ST}+\boldsymbol{Y}_{TR}. \quad (10)$$

The unbalanced admittance is

$$\boldsymbol{A}=\left|\boldsymbol{A}\right|e^{j\varphi}=-(\boldsymbol{Y}_{ST}+\alpha\boldsymbol{Y}_{TR}+\alpha^*\boldsymbol{Y}_{RS}) , \quad (11)$$

where α=1e$^{j120^\circ}$ and α^*=1e$^{-j120^\circ}$. Having these admittances the three-phase current vector can be decomposed into mutually orthogonal components as

$$\mathbf{i}=\begin{bmatrix}i_R & i_S & i_T\end{bmatrix}^{\mathrm{T}}=\mathbf{i}_a+\mathbf{i}_r+\mathbf{i}_u. \quad (12)$$

As shown in [10] the actual admittances at the point of measurement do not need to be known. The value of these admittances can change as the *N*-sample moving window of the RDFT advances. Therefore, the admittances are considered as time varying quantities denoted by the ~ symbol. Having these two admittances the time varying equivalent admittance is given by

$$\tilde{\boldsymbol{Y}}_{\boldsymbol{e}}=\tilde{G}_e+j\tilde{B}_e=\tilde{\boldsymbol{Y}}_{ST}+\tilde{\boldsymbol{Y}}_{TR}=\frac{\tilde{\boldsymbol{I}}_S}{\tilde{\boldsymbol{U}}_{ST}}+\frac{\tilde{\boldsymbol{I}}_R}{\tilde{\boldsymbol{U}}_{RT}}, \quad (13)$$

and the time varying unbalanced admittance is given by

$$\tilde{\boldsymbol{A}}=\left|\tilde{\boldsymbol{A}}\right|e^{j\tilde{\varphi}}=-(\tilde{\boldsymbol{Y}}_{ST}+\alpha\tilde{\boldsymbol{Y}}_{TR}) . \quad (14)$$

A main advantage can now be seen with regard to the phase error, $\Delta\varphi(k)$, introduced by frequency deviation error of the RDFT. Note that the phase error will be canceled in the admittances calculation since $\Delta\varphi(k)$ exists in both phase expressions for the voltage and current, thus, their difference will exclude the phase error $\Delta\varphi(k)$. Therefore, only a small error will be introduced in the magnitude of the admittance calculations due to the magnitude error factor λ.

c. Effect on current reference signal

The time varying equivalent and unbalanced admittances can be used to generate current reference signals. A three-wire system is assumed so that only two phases are needed. With the time varying equivalent and unbalanced admittances, current components can be generated as shown in [6] with expression

$$\begin{bmatrix}i_{Ra}\\ i_{Sa}\end{bmatrix}=\sqrt{2}\tilde{G}_e\begin{bmatrix}\mathrm{Re}\{\tilde{U}_R\}\cos\omega_{1g}k-\mathrm{Im}\{\tilde{U}_R\}\sin\omega_{1g}k\\ \mathrm{Re}\{\tilde{U}_S\}\cos\omega_{1g}k-\mathrm{Im}\{\tilde{U}_S\}\sin\omega_{1g}k\end{bmatrix} \quad (15)$$

for active current in phases R and S,

$$\begin{bmatrix}i_{Rr}\\ i_{Sr}\end{bmatrix}=\sqrt{2}\tilde{B}_e\begin{bmatrix}-\mathrm{Re}\{\tilde{U}_R\}\sin\omega_{1g}k-\mathrm{Im}\{\tilde{U}_R\}\cos\omega_{1g}k\\ -\mathrm{Re}\{\tilde{U}_S\}\sin\omega_{1g}k-\mathrm{Im}\{\tilde{U}_S\}\cos\omega_{1g}k\end{bmatrix} \quad (16)$$

for the reactive currents, and

$$\begin{aligned}\begin{bmatrix}i_{Ru}\\ i_{Su}\end{bmatrix}&=\sqrt{2}\begin{bmatrix}(\mathrm{Re}\{\tilde{A}\}\mathrm{Re}\{\tilde{U}_R\}-\mathrm{Im}\{\tilde{A}\}\mathrm{Im}\{\tilde{U}_R\})\cos\omega_{1g}k\\ (\mathrm{Re}\{\tilde{A}\}\mathrm{Re}\{\tilde{U}_T\}-\mathrm{Im}\{\tilde{A}\}\mathrm{Im}\{\tilde{U}_T\})\cos\omega_{1g}k\end{bmatrix}\\ &\quad-\begin{bmatrix}(\mathrm{Re}\{\tilde{A}\}\mathrm{Im}\{\tilde{U}_R\}+\mathrm{Im}\{\tilde{A}\}\mathrm{Re}\{\tilde{U}_R\})\sin\omega_{1g}k\\ (\mathrm{Re}\{\tilde{A}\}\mathrm{Im}\{\tilde{U}_T\}+\mathrm{Im}\{\tilde{A}\}\mathrm{Re}\{\tilde{U}_T\})\sin\omega_{1g}k\end{bmatrix}\end{aligned} \quad (17)$$

for the unbalanced currents.

Unfortunately, even though the calculated values of *Ge*, *Be*, and $\boldsymbol{A}$ have negligible error even for large frequency deviations, the CRMS values of the voltages computed by the RDFT have a non-negligible phase error. Because the RDFT calculation of the measured voltage contains a phase error given by (9) the reference currents generated by the current reconstruction algorithm will also contain a phase error. However, unlike the voltage phase error, the current phase error does not vary in time. This can be seen by applying (7) to the expression for current (15). For phase R this gives the expression

$$\begin{aligned}i_{Ra}&=\sqrt{2}\tilde{G}_e\lambda U\sin[(\Delta\omega k)-\delta+\varphi]\cos\omega_{1g}k\\ &\quad+\sqrt{2}\tilde{G}_e\lambda U\cos[(\Delta\omega k)-\delta+\varphi]\sin\omega_{1g}k .\\ &=\sqrt{2}\tilde{G}_e\lambda U\sin[\omega_{1g}k+\Delta\omega k-\delta+\varphi]\end{aligned} \quad (18)$$

Similarly, for reactive current phase R we obtain

$$
\begin{aligned}
i_{Rr} &= -\sqrt{2}\tilde{B}_e \lambda U \sin[(\Delta\omega k) - \delta + \varphi]\sin\omega_{1g}k \\
&\quad + \sqrt{2}\tilde{B}_e \lambda U \cos[(\Delta\omega k) - \delta + \varphi]\cos\omega_{1g}k \,. \\
&= \sqrt{2}\tilde{B}_e \lambda U \cos[\omega_{1g}k + \Delta\omega k + \delta + \varphi]
\end{aligned} \tag{19}
$$

Finally, the unbalanced current is

$$
i_{Ru} = \sqrt{2}\lambda U \begin{bmatrix} \mathrm{Re}\{\tilde{A}\}\sin(\omega_{1g}k + \Delta\omega k - \delta + \varphi) \\ +\mathrm{Im}\{\tilde{A}\}\cos(\omega_{1g}k + \Delta\omega k + \delta + \varphi) \end{bmatrix}. \tag{20}
$$

Thus, the reference current has the same frequency as the voltage, $\omega_{1g} + \Delta\omega$, but each component contains a phase error equal to δ. This introduces a phase shift in the reference generator output relative to the desired phase setting. However, the CPC equivalent admittance computed at the measurement terminals is computed correctly due to cancellation of the phase error in the admittances calculation. Fortunately, the correct phase of the admittances allows the correction of the reference current phase error.

Reference signal generator

A generalized reference generator (RSG) that allows compensation applications in addition to active rectification under non-ideal supply voltage and frequency variation is presented here. As in [6], in order to provide flexibility of the compensation objectives the current control reference signal is expressed as a linear form

$$
\boldsymbol{j}^* = K_r \boldsymbol{i}_{Mr1} + K_u \boldsymbol{i}_{Mu1} + K_h \boldsymbol{i}_{Mh} + \boldsymbol{i}_{Ca} \,, \tag{21}
$$

where K_r, K_u and K_h are scaling coefficients of the reactive, unbalanced and harmonic components respectively and current measurement input of the reference generator is denoted as $\boldsymbol{i}_M$. Also, only the equivalent conductance of the fundamental is computed and not the equivalent conductance. Therefore, in cases where voltage distortion is present the supply current RMS value will always be higher than its minimum due to the presence of scattered current. However, the supply current will be sinusoidal if K_h=1.

One condition of the non-ideal supply considered here is asymmetry. In the case that the supply is asymmetrical, voltage sequence must be separated in order for unbalanced current to have meaning. In order for the converter to inject or draw balanced currents, only positive-sequence voltage is used by the reference signal generator. Thus, active component of the converter, $\boldsymbol{i}_{Ca}$, is equal to

$$
\boldsymbol{i}_{Ca} = \frac{P_{DC} + \Delta P_{sc} + \left\|\boldsymbol{i}_{a1}^N\right\|\left\|\boldsymbol{u}_1^N\right\| + \sum_{n\in N_h}\left\|\boldsymbol{i}_{an}\right\|\left\|\boldsymbol{u}_n\right\|}{\left\|\boldsymbol{u}_1^P\right\|^2}\boldsymbol{u}_1^P \,, \tag{22}
$$

where P_{DC} is power drawn by any DC load connected to the DC bus of the converter and ΔP_{sc} are losses of the converter. Superscripts 'P' and 'N' denote positive and negative sequences respectively. Active component of the converter is adjusted by the DC bus voltage control as needed to satisfy the power balance. A simplified block diagram of the reference signal generation strategy is shown in Fig. 2.

A main feature of this RSG as compared with that in [5] is the use of voltage positive sequence as well as the additional RDFT and CPC based current decomposition that allows removal of the phase error present in expressions (18) - (20). This second set, shown in the dashed box, provides a correct value of the equivalent and unbalanced admittances that can be used to correct the phase error in the current. The addition of a control loop to force B_e and $\boldsymbol{A}$ equal to the desired set-points will remove the phase error introduced into the current reconstruction algorithm by the RDFT of the measured supply voltage.

Simulation results

In order to validate the proposed reference signal generator a three-phase grid connected converter system for both compensation and rectifier applications was designed and several tests were performed in simulation. A diagram of the test system is shown in Fig. 3. The test system is composed of an AC load bank in parallel with the converter for compensation applications and a DC load connected to the VSC DC bus for rectifier applications. The AC load bank consists of a linear RL load that can be unbalanced. Test system parameters are provided in Table 1. The VSC of the test system has the same control as described in [5] except that the reference signal generator is replaced with the proposed one shown in Fig. 2.

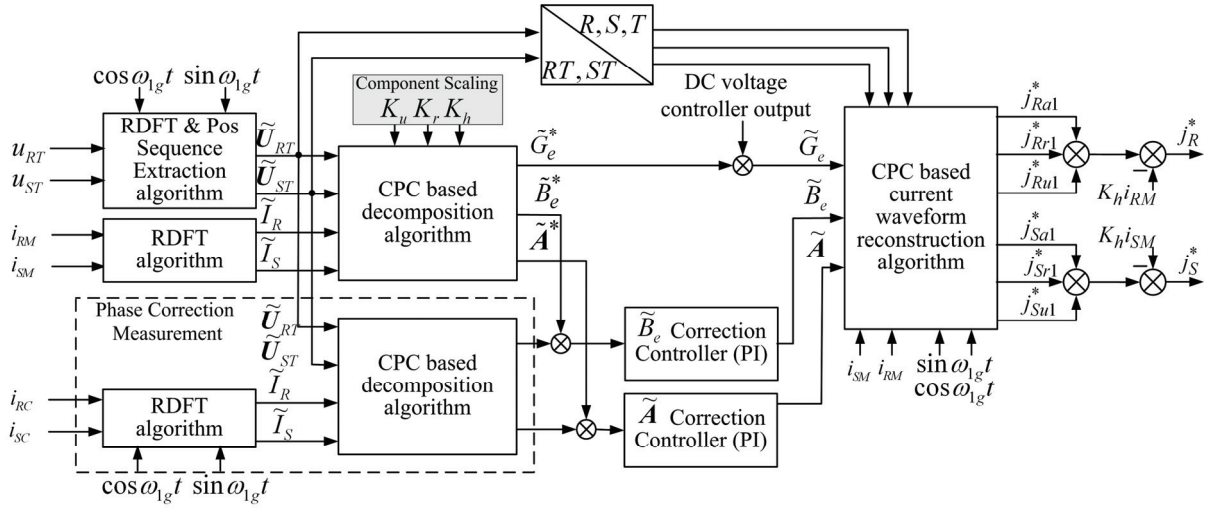

Fig. 2. Proposed reference signal generator without synchronization for grid-connected VSCs.

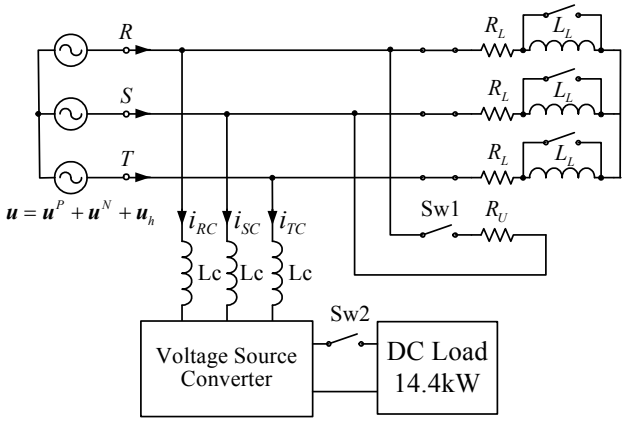

Fig. 3. Test System.

The supply voltage may contain both asymmetry as well as harmonic distortion in addition to frequency variation and is expressed as

$$\boldsymbol{u} = \boldsymbol{u}^P + \boldsymbol{u}^N + \boldsymbol{u}_h , \tag{23}$$

where $\boldsymbol{u}^{\mathrm{P}}$ is a positive sequence sinusoidal voltage vector and $\boldsymbol{u}^{\mathrm{N}}$ is a negative sequence sinusoidal voltage vector with line-to-neutral voltage at terminal R equal to

$$u_R^P = \sqrt{2}U^P \cos\omega_1 t \qquad u_R^N = \sqrt{2}U^N \cos\omega_1 t \ . \tag{24}$$

Distorted component of the voltage is given by $\boldsymbol{u}_{\mathrm{h}}$ with line-to-neutral voltage at terminal R equal to

$$u_{Rn} = \sqrt{2}XU^P \cos n\omega_1 t \tag{25}$$

with RMS value of X percent of the positive sequence fundamental.

Table 1. Parameters of the Test System.

AC Load Resistance, R_L	1.16Ω
AC Load Inductance, L_L	5mH
Unbalanced Load, R_u	16 Ω
Supply nominal frequency	60Hz
Coupling inductance, Lc	1.0mH
DC bus capacitor	2700μF
DC bus reference voltage	700V
VSC Switching Frequency	12KHz

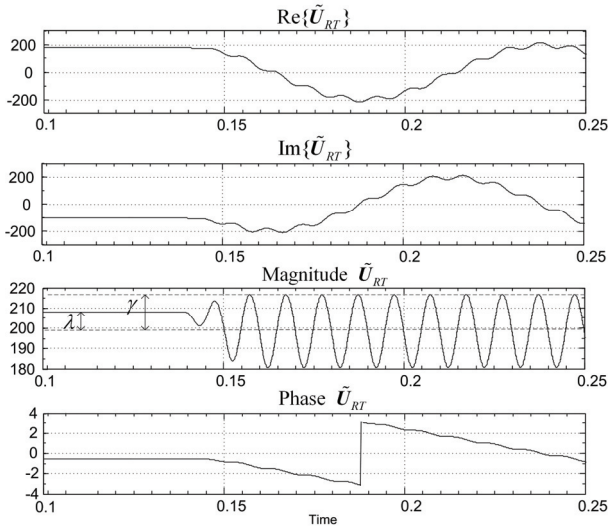

Fig. 4. CRMS value of positive sequence of voltage U_{RT} before and after -10Hz frequency step change without reactive current control loop.

Simulation results during a frequency step change of -10Hz are shown for various test cases. In all cases at time t=8.3/60 the frequency step change of –10Hz occurs. Figure 4 shows the real and imaginary components as well as magnitude and phase of the positive sequence fundamental of voltage U_{RT} computed by the RDFT before and after the frequency step change.

Three simulation test cases demonstrate the performance of the proposed reference signal generator for various system conditions.

a. Compensation with sinusoidal asymmetrical supply and linear balanced load

Simulation results are shown for reactive current compensation for a linear load. Switches Sw1 and Sw2 are open at all times and supply asymmetry occurs at t=6/60 seconds with U^P=120 and U^N= U^P/2.

Equivalent Conductance of the load and the converter are shown in Fig. 5. Note that the equivalent conductance of the converter, G_{ec}, is initially small due to power losses, ΔP_{sc}, but increases when the voltage asymmetry occurs. This is because in order to balance the supply current the converter must convert active power of negative sequence at the load into active power of positive sequence at the supply. Equivalent Susceptance and Unbalanced Admittance are shown in Fig. 6.

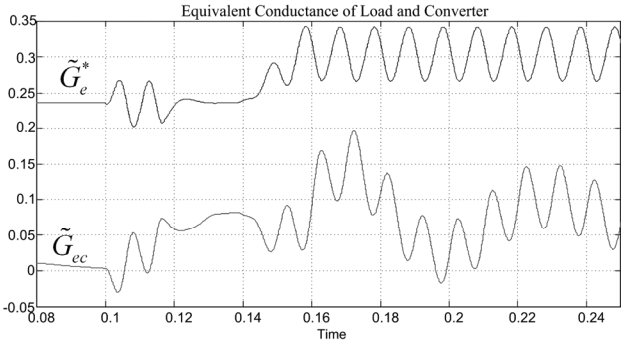

Fig. 5. Equivalent Conductance of the AC load and VSC with voltage asymmetry at t=6/60 and -10Hz frequency step at t=8.3/60.

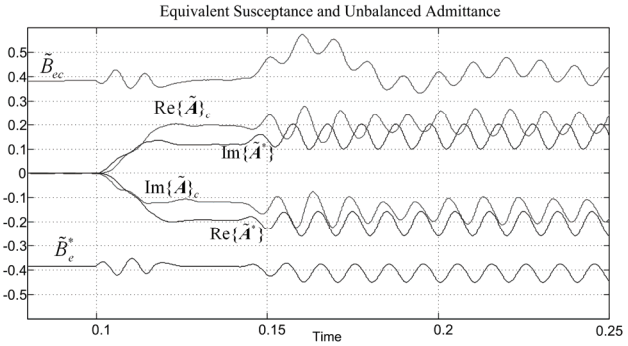

Fig. 6. Equivalent Susceptance and Unbalanced Admittance of the AC load and VSC with voltage asymmetry at t=6/60 and -10Hz frequency step at t=8.3/60.

Equivalent Susceptance of the converter, B_{ec}, is regulated to the set-point that in this case is equal to the negative of the measured load reactive power. Unbalanced admittance is also regulated to the set-point. After the frequency change, the phase shift in the generated currents means that both the active current and reactive current reference currents both contain active and reactive components. The correction controllers ensure that the active and reactive power of the total reference current are

correct. Therefore, the reference admittances are correct, as shown in Fig. 6, even after the frequency step change. However, the large ripple in this case does cause slight distortion of the converter current. The supply voltage, compensated supply currents and load currents are shown in Fig 7. Figure 8 shows supply voltage and current for Phase *R*. The phase shift caused by the frequency step change can be seen but is corrected within two cycles.

b. Supply of a DC load and compensation with sinusoidal asymmetrical supply and linear unbalanced load

Simulation results are shown for compensation of a linear but unbalanced load along with a DC load. In this case the voltage is initially asymmetrical with U^P=120 and U^N=U^P/2 as in the previous case. Switches Sw1 and Sw2 are closed at all times

The Equivalent Conductance does not change since the active current controller is regulating the DC bus voltage at the set-point by maintaining the required DC load active power as well as negative sequence active power of the fundamental in the AC load.

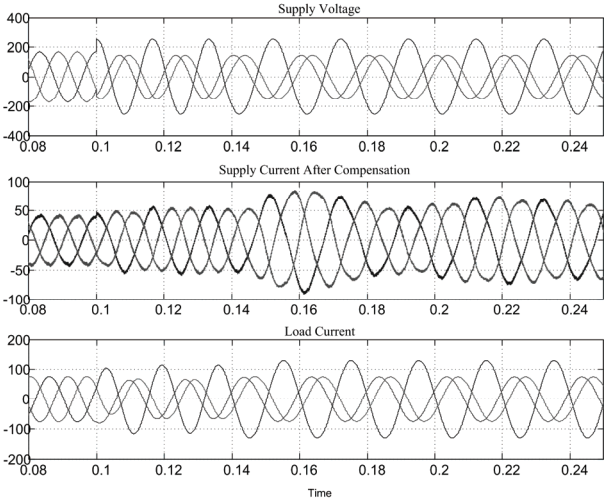

Fig. 7. Supply voltage, supply current and load current.

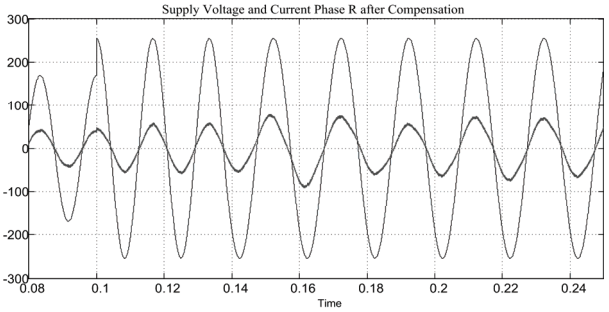

Fig. 8. Phase R supply voltage and supply current.

However, as previously, when the frequency change occurs the Equivalent Susceptance of the converter must change due to the phase error introduced into the current reference. Equivalent Susceptance and Unbalanced Admittance of the converter are regulated to the set-points as shown in Fig. 9. The supply voltage and the compensated supply current in steady-state after the de-synchronization of –10Hz are shown in Figure 10 (a) and (b) respectively.

c. Supply of a DC load and compensation with non-sinusoidal asymmetrical supply and linear unbalanced load

Simulation results are shown having all load conditions the same as in Section IV *B*. However, in this case the voltage is heavily distorted with a 5th order harmonic equal to 10% of the fundamental, X=0.1, in addition to asymmetrical with U^P=120 and U^N= U^P/2.

The supply voltage, supply currents and load currents are shown in Fig. 11. As expected, the performance is not effected by the voltage distortion since the RDFT as computed using (1) extracts only the fundamental.

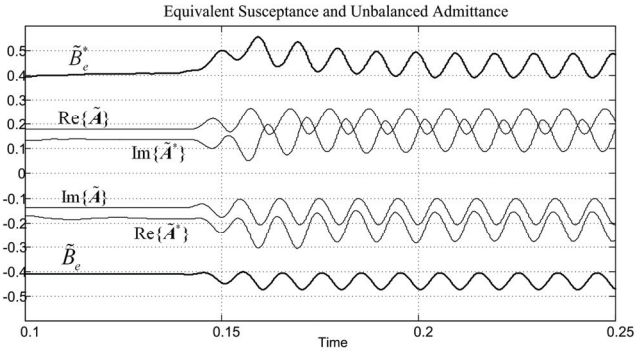

Fig. 9. Equivalent Susceptance and Unbalanced Admittance before and after -10Hz frequency step change for both load and corrected reference outputs.

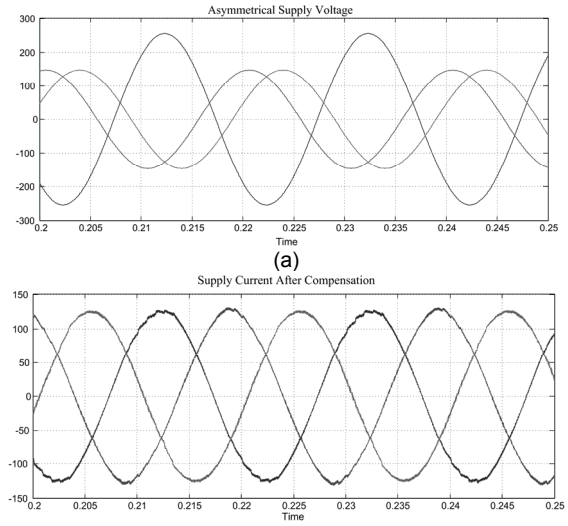

Fig. 10. Supply voltage (a) and compensated supply current (b) after -10Hz frequency step change.

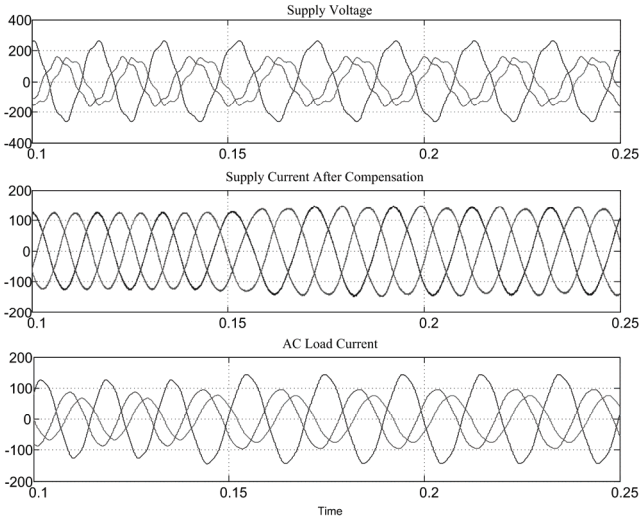

Fig. 11. Distorted and asymmetrical supply voltage, supply current and load current.

Conclusions

A CPC based converter control method that does not require direct supply synchronization and is suitable for systems with non-ideal supply voltages and high frequency variation has been developed. The reference signal generator is almost immune to frequency variations with only very small high frequency ripple resulting from large frequency deviation from the nominal set-point. Furthermore, it is not possible for the developed control scheme to lose phase-lock since it does not require direct supply synchronization to operate. It also performs well under supply voltage asymmetry and distortion. The converter rating must be increased under such conditions since active power at harmonic frequencies or negative sequence active power at the fundamental are converted to positive sequence active power at the fundamental frequency.

REFRENCES

[1] R. Teodorescu, F. Blaabjerg, M. Liserre, and P. Loh, "Proportional-resonant controllers and filters for grid-connected voltage-source converters, IEE Proc. Electr. Power App. Vol. 153, No. 5, Sept. 2006, pp. 750-762.

[2] Timbus, M. Ciobotaru, R. Teodorescu and F. Blaabjerg, "Adaptive Resonant Controller for Grid-Connected Converters in Distributed Power Generation Systems," Twenty-First Annual IEEE Applied Power Electronics Conference and Exposition, (APEC '06), 19-23 March 2006.

[3] M. Liserre, R. Teodorescu, F. Blaabjerg, "Multiple Harmonics Control for Three-Phase Grid Converter Systems With the Use of PI-RES Current Controller in a Rotating Frame," IEEE Trans. on Power Electronics, Vol. 21, No. 3, May 2006, pp. 836-841.

[4] D. N. Zmood, D. G. Holmes, "Stationary Frame Current Regulation of PWM Inverters with Zero Steady-State Error," IEEE Trans. on Power Electronics, Vol. 18, No. 3, May 2003, pp. 814-822.

[5] H. L. Ginn III, G. Chen, "Control Method for Voltage Source Converters in Systems with High Frequency Variability", Proceedings of the 8th International IEEE Conference on Power Electronics and Drive Systems (PEDS'09), November 2009, pp. 1008-1013.

[6] H. Ginn, G. Chen, "Flexible Active Compensator Control for Variable Compensation Objectives", IEEE Trans. on Power Electronics, Vol. 23, Issue 6, Nov. 2008, pp. 2931 – 2941.

[7] Hatem A. Darwish and Magdy Fikri, "Practical Considerations for Recursive DFT Implementation in Numerical Relays", *IEEE Trans. on Power Delivery*, Volume 22, Issue 1, Jan. 2007, pp. 42 – 49.

[8] J. A. Rosendo Macfas, A. Gomez Exposito, "Efficient Moving-Window DFT Algorithms," *IEEE Trans. On Circuits and Systems II: Analog and Digital Signal Processing*, Vol. 45, No. 2, February 1998.

[9] L. S. Czarnecki, "Orthogonal decomposition of the current in a three-phase nonlinear asymmetrical circuit with nonsinusiodal voltage," *IEEE Trans. Instrum. Meas*., Vol. IM-37, March 1988, pp. 30-34.

[10] L. S. Czarnecki, "Power Theory of Electrical Circuits with Quasi-Periodic Waveforms of Voltages and Currents," *ETEP*, Vol. 6, No. 5, September/October 1996.

***Author**: dr inż. Herbert Ginn, University of South Carolina, Dept. of Electrical Engineering, Swearingen Engineering Center 3A13, Columbia, SC 29208, U.S.A, E-mail: ginnhl@cec.sc.edu*